Evaluation of Five Algorithms for Mapping Brain Cortical Surfaces

Simon Fristed Eskildsen Lasse Riis Østergaard

Department of Health Science and Technology
Aalborg University
Fredrik Bajers Vej 7D, 9220 Aalborg East, Denmark
se@hst.aau.dk

Abstract

With the increasing resolution and contrast of brain imaging devices automatic segmentation and quantification of the human cerebral cortex have grown popular for morphological analyses. The tightly folded cortex is often modeled with surfaces in 3D, and morphological features, such as the cortical thickness, can be calculated. In order to average and compare such morphological features within groups of subjects, mappings between the highly diverse cortical surfaces are needed. In this paper we evaluate five algorithms for mapping between discrete polygonal surfaces of cortices. Among the evaluated algorithms we include a new algorithm based on a functional expressing similarity between geometrical features. Four numerical mapping criteria, a landmark test, and statistical maps are used to evaluate the mapping algorithms. We show that the accuracy of manually placed landmarks are difficult to reproduce automatically, and the choice of mapping algorithm impacts the conclusions drawn from statistical maps generated by use of the algorithm. In terms of landmark accuracy, a spherical mapping approach with non-linear optimization is shown to be the best of the tested algorithms.

1 Introduction

Morphological analysis of the human cerebral cortex from in-vivo medical images plays an important role in the investigation of various neurological disorders, such as schizophrenia and dementia [18, 6]. Increasing effort is being put into measuring cortical morphological changes over time and differences between populations. Magnetic resonance imaging (MRI) provides excellent structural information of the cerebral tissues, and surface reconstructions of the cortex from MRI have grown popular for studying morphological features, such as cortical thickness, area, and patterns of the cortical folds. During the last decade several surface reconstruction algorithms have been proposed [7, 14, 17, 21, 9, 34], and several ways to obtain cortical thickness measurements and other features from cortical surfaces have been developed [24, 28]. Usually the cortical surfaces are approximated by discrete polygonal meshes, and cortical features are calculated at each vertex provided a reasonably uniform distribution of vertices across the surface. To measure morphological differences between subjects one can average the measurements over the entire cortex or within specified regions, but to exploit the detailed map of measurements provided by high resolution surfaces and be able to detect focal differences a point correspondence between cortical surfaces is required. Such a mapping must preserve anatomical landmarks across subjects in order to reliably compare measurements, i.e. it does not make sense to compare the top of a fold (gyrus) on one surface with the bottom of a fold (sulcus) on another surface. Because of the high diversity of folding patterns across individual cortices, such a mapping is far from trivial.

2 Background

Several methods to solve the cortical mapping problem have been proposed. A popular approach is to parameterize the cortical surface by mapping the surface into a canonical space and solve the correspondence problem in this space. Often the unit sphere is used, as it is topologically equivalent to the cortical surface and provides an attractive coordinate system for easy parameterization [13]. Utilizing the Riemann mapping theorem on manifold surfaces [1] several approaches have been proposed to conformally map the cortical surface to a sphere [31, 16, 19, 26, 25, 23]. Also other canonical spaces have been used for parameterization, such as an ellipsoid and the 2D plane [33]. The latter, so-called flat maps, require cuts in the closed surface to be able to map the surface to the plane. Consistent cuts are hard to automate, thus requiring manual intervention.

After parameterization of cortical surfaces the correspondence between vertices can be obtained by registration of the surfaces in the canonical space using the preserved geometrical features as similarity measure. This registration is usually a non-linear warp because of the highly irregular folding patterns [12, 35].

The mapping onto a canonical space introduces geometrical distortion in the surface, and even though work has been focused on minimizing the distortion in the conformal mapping [23] it remains a problem for the subsequent parameterization and registration. Creating flat maps introduces more geometrical distortion than the spherical approach and alters the topology thus partly destroying geodesic relations between vertices [12]. Several methods constrain the mapping using landmark curves [33, 16, 25, 29]. These are often manually defined, but methods have been proposed to automate identification of landmark curves [15, 28, 22], though it is hard to do consistently [4].

Another group of methods try to solve the correspondence problem without the intermediate step of mapping to a canonical space. One family of such methods is derived from the iterative closest point method (ICP) [5, 2]. Apart from variations over the simple closest point method, several methods combine ICP with point feature registration [10, 27]. Others approach the problem by finding a direct mapping using partial differential equations (PDE) [29] or diffeomorphisms [32].

Common for the mapping approaches described above is the preservation of intrinsic vertex configuration, except from the cuts introduced when creating flat maps. This may seem important, as these geometric properties reflect the underlying cytoarchitecture of the cortex. However, when mapping between cortices with very different cortical folding patterns, this constraint can be relaxed to better match morphological features. A feature based method disregarding the intrinsic vertex configurations was proposed by Spjuth et al. [30]. They used a similarity functional based on mean curvature, surface normals, and Euclidean distance to find corresponding vertices between surfaces after an initial, global, affine registration. The method allows several vertices to map to the same target vertex while other vertices are left without mapping. Thereby information is lost. To retain information, the optimal solution is a bijection between the surfaces only mapping between similar anatomical points. When a vertex to vertex correspondence is needed the mapping cannot be a bijection if the two cortex surfaces have different number of vertices. However, one can try to approximate a bijection by having unique projections for as many vertices as possible.

As described above a variety of algorithms for solving the cortical mapping problem have been proposed. However, to the best of our knowledge, comparisons of the different approaches have not been carried out. In this paper we propose a new algorithm for the problem of finding vertex correspondence between surfaces with different vertex counts and evaluate the performance of the proposed algorithm along with a selection of other mapping algorithms.

3 Proposed Mapping Algorithm

The proposed algorithm for mapping a source surface to a target surface is inspired by Spjuth et al. [30], and it uses the same similarity features, but seeks to optimize the number of unique mappings, thereby approximating a bijection as close as possible. The algorithm initially aligns the two surfaces with a rigid transformation found by center of mass normalization followed by ICP optimization [5]. The method for finding a vertex to vertex correspondence from source to target surface uses a cost functional J. The cost of mapping between source vertex i and target vertex j is given by

$$J(i,j) = \alpha e^{c(i,j)} + \beta e^{n(i,j)} + \gamma e^{d(i,j)} \qquad (1)$$

where c is the absolute difference in normalized mean curvature at the vertices, n is the normalized angle between the vertex normals, d is the normalized Euclidean distance between the vertices, and α, β and γ are weights. This cost functional is sought minimized per source vertex by the following algorithm:

Definitions:
V_s is the set of source vertices.
V_t is the set of target vertices.
t_c is the cost threshold any mapping must be below.
t_m is the maximum number of mappings allowed to the same target vertex.
N_s is the set of source vertices without a mapping.
N_t is the set of target vertices with number of mappings $< t_m$.
Initial conditions: $N_s = V_s$, $N_t = V_t$, and $t_m = 1$.

1. For each vertex in N_s find the vertex in N_t with the lowest mapping cost defined by J.
2. For each vertex in V_t where number of mappings $> t_m$ remove highest cost mappings until number of mappings $= t_m$. Update N_s and N_t.
3. Repeat 1 until no mappings are found with a cost $< t_c$, or either N_s or N_t is empty.
4. If N_s is non-empty, set $N_t = V_t$, $t_m = t_m + 1$ and repeat from 1.

We designate the algorithm iterative closest feature (ICF), because of its use of point features and iterative behavior. The weights in the cost functional were found by repeated trials of mapping between two simple phantom surfaces where the true mapping was known. The found weights were $\alpha = 3.7$, $\beta = 1.1$, and $\gamma = 2.7$.

4 Algorithms Selected for Comparison

Apart from the proposed mapping algorithm we wanted to evaluate a handful of typical algorithms to find their strengths and weaknesses. The following algorithms were included in the evaluation:

- Iterative closest point (**ICP**). The basic ICP algorithm [5] to compare with a simple and "naive" approach.
- **Feature**. The method by Spjuth et al. [30] was included as this method is similar to the proposed algorithm but without the iterative behavior.
- Iterative closest feature (**ICF**). The proposed method as described in section 3.
- Spherical **Warp**. This is the method used in FreeSurfer to register a cortical surface to a "canonical" surface [12, 13]. Source and target surfaces are mapped to the unit sphere (figure 1) and the folding patterns are aligned using a warp minimizing the mean squared difference between the average convexity [13]. This method is included as the algorithm is freely available and the spherical mapping introduces less metric distortion than other mapping methods [20]. To obtain a vertex correspondence map, the geodesic closest points are used between two surfaces registered to the canonical surface provided by FreeSurfer.
- **Spherical**. A method where source and target surfaces are mapped to a sphere and corresponding points are found by rotations of the source surface optimizing curvature correlation. The method is similar to the approach described by Fischl et al. [12], but instead of the final non-linear warp a rigid optimization is performed iteratively in a multi-scale manner. The spherical mapping was done using FreeSurfer [7], while the subsequent optimization was implemented locally. As in the warp approach described above, a vertex correspondence map is obtained by the geodesic closest points between the two surfaces after optimization.

The following section describes how the five mapping algorithms were evaluated.

5 Mapping Evaluation

Performance of the algorithms was tested using 10 cortical surfaces extracted by the FreeSurfer software [7] from T1 weighted MRI scans (1.5 Tesla, 30°flip angle, TR/TE=18/10 ms, isotropic 1 mm voxels) from young healthy subjects. FreeSurfer produces surfaces of the inner and outer boundary of the cortex for each hemisphere separately. Surfaces of the outer cortical boundary of left hemispheres only were used in the evaluation, as brain symmetri properties suggest that either hemisphere is representative for the cortical variation, and the mapping algorithms are expected to perform equally well on both hemispheric surfaces. Surfaces generated by FreeSurfer are triangular meshes with spherical topology and have arbitrary number of vertices, thus they are well-suited for testing the algorithms described here. The 10 extracted left cortical surfaces had on average 148k$\pm$8k vertices. The distribution of vertices were assumed similar for the generated surfaces. All 10 cortical surfaces were in turn used as target for mapping the other nine surfaces, thus resulting in 90 mappings in total used in the evaluation.

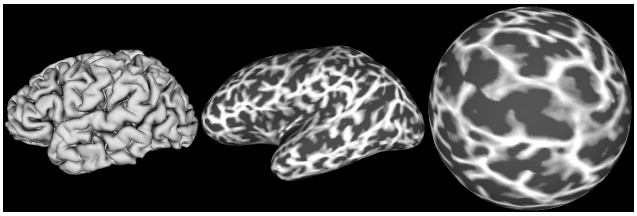

Figure 1. From cortex surface to sphere. Left: Original cortical surface. Middle: Inflated surface with curvature values superimposed. Right: Surface mapped to a sphere with curvature values superimposed.

The optimal corresponding target vertex for any given source vertex can be sought even though this means that two distinct vertices may map to the same vertex on the target surface. It is desirable to map to as many vertices on the target surface as possible to retain information, i.e. the image of the mapping must cover as much of the target surface as possible. The higher coverage of the target surface the better approximation of a bijection between the surfaces. Therefore, one criterion for a good mapping is the percentage of vertices on the target surface that are used as correspondence points for vertices on the source surface, i.e. the coverage of the target surface. If the source surface has less vertices than the target surface full coverage is not possible. Therefore the coverage error, C, is defined as:

$$C = 1 - \frac{|M_t|}{min(|V_s|, |V_t|)}, \tag{2}$$

where M_t is the set of target vertices with a mapping, and V_s and V_t are the same as in section 3. Thus a full coverage results in $C = 0$ while mappings with less coverage have higher values with a theoretical upper limit of $C = 1$.

Increasing the vertex count of the source surface provides better conditions for a good coverage. However, a source surface with twice as many vertices as the target surface may provide full coverage of the target surface with-

out being considered a good mapping if for instance a large portion of source vertices map to the same target vertex. Therefore, another criterion for a good mapping is the mean square number of mappings per target vertex normalized by the squared source/target vertex count ratio. The multiple mapping error, M, is defined as:

$$M = \frac{\frac{1}{|V_t|}\sum_{j\in V_t} m_j^2}{(\frac{|V_s|}{|V_t|})^2} - 1 = \frac{|V_t|\sum_{j\in V_t} m_j^2}{|V_s|^2} - 1 \qquad (3)$$

where m_j is the number of mappings to vertex j of the target surface. If $M = 0$ the mapping is optimal with regard to the criterion, while higher values of M signal worse mappings with a theoretical upper limit of $M = |V_t| - 1$.

When mapping between surfaces we expect that patches of the source surface are mapped to patches of similar size on the target surface. We introduce a third criterion aiming at evaluating this property. For each vertex i on the source surface we determine the geodesic distances to the neighbors along the target surface after applying the map, where the geodesic distance is calculated as the minimum edge length between vertices (Dijkstra's algorithm [8]). Optimally, this distance should be the same as on the source surface when surfaces have equally distributed vertices. We calculate the geodesic error at vertex i as:

$$\phi(i) = \frac{1}{|N(i)|}\sum_{j\in N(i)} |g(m(i), m(j)) - g(i, j)| \qquad (4)$$

where $N(i)$ is the set of neighboring vertices to vertex i on the source surface, $g(i, j)$ is the geodesic distance between i and neighbor j, while $g(m(i), m(j))$ the geodesic distance between these vertices after the mapping. The density evaluation criteria, D, is defined as the average of the geodesic errors:

$$D = \frac{1}{|V_s|}\sum_{i\in V_s} \phi(i) \qquad (5)$$

A mapping with good preservation of source surface patches has a small D with a theoretical minimum of $D = 0$ for the perfect preservation. This metric is affected if the vertex distributions of the two surfaces are highly irregular. For this reason, similar distributions of the surfaces are assumed.

Finally, we wanted to evaluate if vertices are mapped between similar topographical areas. To quantify this we define a topography criterion, T, as the average difference in mean curvature before and after mapping to the target surface:

$$T = \frac{1}{|V_s|}\sum_{i\in V_s} |\rho(i) - \rho(m(i))| \qquad (6)$$

where $\rho(i)$ is the mean curvature at vertex i and $m(i)$ is the mapping of vertex i (the target vertex). Curvature values are normalized to the interval $[-1 : 1]$, thus the topography criterion has values in $[0 : 2]$ with theoretical extrema.

The four criteria described above are all quantitative approaches to evaluating the mapping between cortical surfaces. To add a more qualitative approach we performed a landmark test to evaluate the algorithms' performance in mapping to the same anatomical landmarks between different cortical surfaces. Six landmarks were identified manually on all 10 cortical surfaces of the left hemisphere. Landmarks were placed by labeling vertices spanning areas of 1-5 mm^2. The selected anatomical landmarks were the temporal pole (TP) at the anterior end of the superior temporal gyrus, the supramarginal gyrus (SG) at the posterior end of the lateral sulcus, the cuneus (Cun) where the parieto-occipital sulcus meets the calcarine sulcus, the posterior part of gyrus rectus (GR), the most superior part of the post central gyrus (PCG), and the cingulate gyrus (CG) at the anterior end of the cingulate sulcus. These anatomical locations were used as they are relatively easy to recognize on the cortical surface, but are still subject of morphological variation. For each mapping the geodesic distances between the mapped landmarks and the manually labeled landmarks were measured and averages over all 90 mappings were calculated.

Finally, we wanted to evaluate the effect of different mapping algorithms on statistical maps, which are often used when measuring cortical thickness. We wanted to test if choice of mapping algorithm would change the conclusions drawn from cortical thickness statistics. The cortical thicknesses of the 10 subjects were therefore mapped to a random target surface and the non-parametric Kruskal-Wallis test [3] was performed at each vertex to test for equality among the mapped values. Furthermore, at each vertex the algorithms were tested against each other using the non-parametric Mann-Whitney-Wilcoxon (MWW) test [3] to evaluate differences between them.

6 Results

The four quantitative evaluation criteria as defined in section 5 were calculated for all 90 mappings. Figure 2 shows the average errors calculated for each algorithm by the evaluation criteria. The results from the landmark test are shown in figure 3.

Table 1 shows the average difference in mean cortical thickness before and after mapping the nine cortices to the randomly selected reference surface. The Kruskal-Wallis test showed that 31% of the vertices were dependent on the mapping algorithm, and the subsequent MWW test revealed that the feature and ICF algorithms were providing similar statistical results, while specifically the spherical rigid approach had areas with conclusions different from the other algorithms (table 2). Figure 4 shows the statistical maps

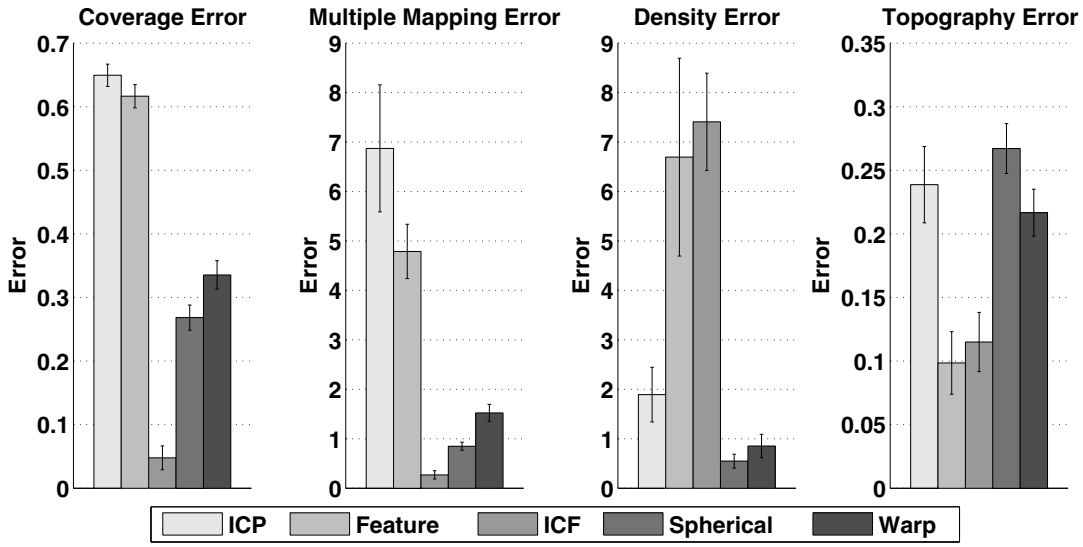

Figure 2. Average errors of mapping with the five tested algorithms between permutations of the 10 cortical surfaces (n=90).

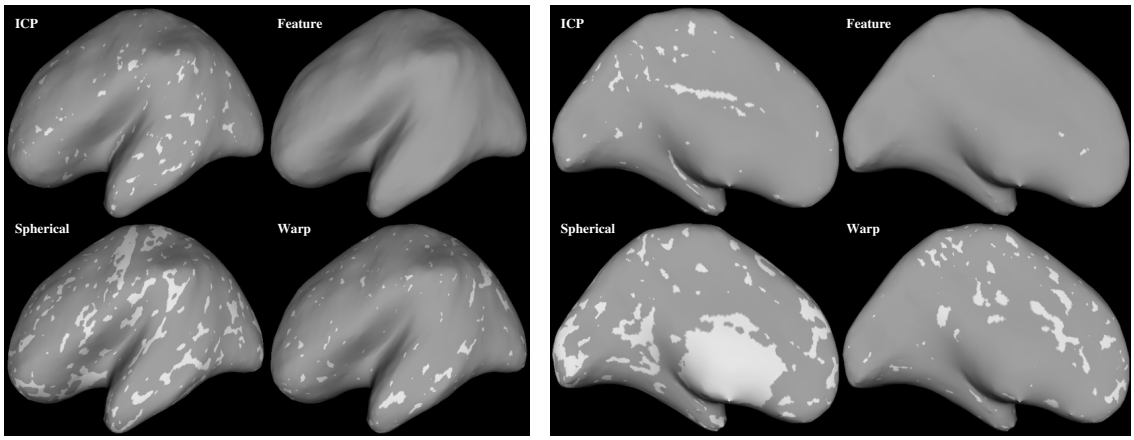

(a) Lateral views (b) Medial views

Figure 4. ICF compared vertex by vertex to the other four mapping algorithms visualized on an inflated reference surface. White areas indicate significant difference ($p<0.05$) in the cortical thicknesses mapped to a vertex.

	Avg. difference (mm)	Paired t-test (p-val)
ICP	-0.10±0.05	<0.01
Feature	0.02±0.03	0.11
ICF	-0.01±0.02	0.06
Spherical	0.00±0.03	0.64
Warp	0.01±0.01	0.13

Table 1. Average difference in mean cortical thickness after mapping.

when comparing the ICF algorithm with each of the other four mapping algorithms using the MWW test.

7 Discussion

Evaluation Metrics

The four evaluation criteria in section 5 were designed to evaluate the behavior of the examined mapping algorithms. Even though the criteria should optimally result in as low

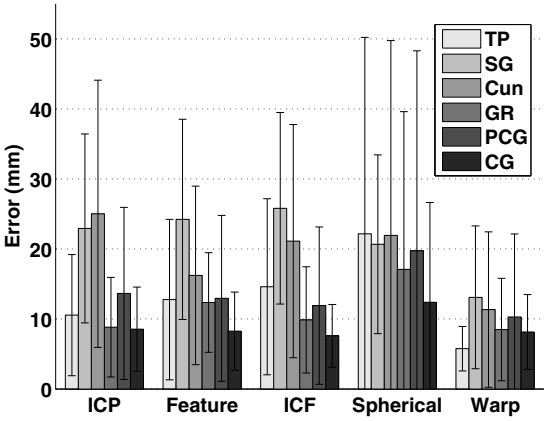

Figure 3. Average distances in mm from mapped landmark to manually labeled landmark of 90 mappings. Landmarks are temporal pole (TP), supramarginal gyrus (SG), cuneus (Cun), gyrus rectus (GR), post central gyrus (PCG), and anterior cingulate gyrus (CG).

values as possible, all criteria cannot be expected to be low because of the highly diverse folding patterns in the surfaces. For example, a low density error, i.e. a good preservation of the intrinsic vertex configurations, will inevitably result in a high topography error, as some vertices are mapped from convexities to concavities and vice versa. Nevertheless, the four criteria are useful for evaluating the algorithms' strengths and weaknesses.

From figure 2 it can be seen that the algorithms behave more or less as expected. The ICP algorithm not surprisingly has relatively high coverage, multiple mapping, and topography errors, while the density error is kept low. This is to be expected as no constraints on multiple mappings or topography preservation are applied, and vertices are kept very compact as only the Euclidean distance is optimized. The feature algorithm as proposed by Spjuth et al. [30] has almost as bad a coverage as the ICP algorithm, but performs better in both the multiple mapping and topography criteria. As expected the density error for the feature algorithm is high, as neighboring vertices are allowed to jump between gyri resulting in long geodesic distances between the mapped vertices. The proposed ICF algorithm behaves approximately similar to the feature algorithm with regard to the density and topography criteria. However, when evaluating the coverage and multiple mapping, it can be seen that this algorithm has the lowest errors among the five evaluated algorithms. This was expected as constraints are enforced to prevent multiple mappings and optimize the coverage.

	Feature	ICF	Spherical	Warp
ICP	6%	3%	24%	14%
Feature	-	0%	22%	6%
ICF	-	-	22%	6%
Spherical	-	-	-	22%

Table 2. Percent vertices of reference surface where the MWW test rejects the hypothesis that the cortical thicknesses come from the same population ($\alpha = 0.05$) for the different mapping algorithms, which means that the mappings influence the conclusion.

The two mapping approaches that use an intermediate step in form of mapping to a sphere have a similar behavior. As expected these algorithms have the lowest density errors among the algorithms, and the multiple mapping errors are also relatively low. This is because the intrinsic vertex configurations are retained during the spherical fitting process. However, the coverage errors are relatively high, and the topography errors are highest among the evaluated algorithms for the rigid spherical approach, while a little lower for the warp approach. This is interesting as the fitting process should minimize the topographical differences between the surfaces. This is a tangible sign of the high diversity of the folding patterns, and that maintaining the intrinsic vertex configurations result in mapping between different topographies. The spherical warp approach which non-linearly should compensate for the highly diverse folding patterns still has high topography errors. This may be explained by the fact that the non-linear fitting is done to an average model instead of the actual target surface. It seems that a combination of the ICF and the spherical approach may provide a nice trade-off between the four mapping criteria.

Landmark Test

Figure 3 reveals that the mapping algorithms are far from perfect when evaluating how well they map between manually labeled landmarks. The error is measured as the geodesic distance to the manually labeled landmark, which means that mapping to a gyrus or sulcus adjacent to the correct results in a large error. From the figure it can be seen that some landmarks are generally more accurately mapped than others no matter the choice of algorithm. The cingulate gyrus are in most cases mapped with a precision of less than 1 cm, and gyrus rectus is also in most cases mapped more accurately than the remaining four landmarks. These two landmarks are both located medially close to the midbrain where cortical variations are less pronounced. The

supramarginal gyrus, which is located in an area of deep sulci and great cortical variability, generally has high errors in all five algorithms. This emphasize the fact that highly convoluted and variable areas are harder to map than less folded areas. The ICP, feature, and ICF algorithms all have similar patterns of landmark errors not significantly ($0.21<p<0.40$) different from each other, which may be due to the similar nature of these algorithms. The spherical approach with the rigid optimization seems to have a more uniform distribution of errors, except for the cingulate gyrus. This can be explained by the rigid optimization. The spherical approach with the non-linear optimization is able to compensate for the high cortical variability, and it results in errors similar to landmarks in areas without great cortical variability, such as the cingulate gyrus and gyrus rectus. Because of the high standard deviations in the landmark errors, it is hard to confidently determine the best mapping algorithm, however, when averaging all landmark errors within each algorithm the spherical warp approach performs significantly ($p<0.001$) better than the other algorithms with an average error of 9.5 ± 9.0 mm, while the spherical rigid approach performs significantly ($p<0.001$) worse with an average error of 19.0 ± 23.4 mm. Further tests should include more subjects and landmarks in concave regions in addition to the convexly located landmarks used here to get a more representative quantification of mapping accuracy.

Statistical Maps

The averaged cortical thickness after mapping to the random reference surface did not change significantly except when using the ICP algorithm (see table 1). However, the generated statistical maps revealed that almost one third of the vertices on the reference surface are dependent on which mapping algorithm is used to map the cortical thickness to the reference. Testing each algorithm against the others revealed that the spherical rigid approach is the algorithm with the largest areas (22% - 24%) of deviating conclusions based on the MWW test (see figure 4 and table 2). Almost no difference is seen between the ICF and feature algorithms while smaller differences is seen between ICF and ICP (3%) and ICF and the spherical warp (6%). As it can be seen from figure 4, 3% is a noticeable portion of a cortex, and may lead to wrong conclusions. This suggests that the impact of the mapping algorithm on the statistical maps is high, and it must be taken into consideration when drawing conclusions from the statistical maps.

Proposed Algorithm

The ICF algorithm extends the simple feature based approach by iteratively approximating a bijection. This is reflected in the quantitative measures of coverage and multiple mapping, where ICF has the lowest errors. However, the algorithm is not more accurate when measuring the distance to the manually placed landmarks, and the statistical maps show no difference between the simple feature based method and the ICF. Though preserving more information, the ICF algorithm does not seem to improve accuracy or change the produced statistical maps.

Both approaches use mean curvature, normal direction, and Eucledian distance for matching vertices. These features do not distinguish between large convex areas, such as the sylvian fissure, and the smaller convexities, such as most of the sulci. Additional features could be included in the cost functional to better map areas of similar sized convexity, e.g. the average convexity as used by FreeSurfer could be used [12, 11]. Also, a term punishing large geodesic distances between vertex neighbors after mapping could be included to compensate for the high density errors. Furthermore, the weights in the cost functional were optimized by a simple phantom surface, and better accuracy may be achieved by optimizing using realistic cortical surfaces.

8 Conclusion

This paper presented a new algorithm for solving the cortical mapping problem and tested it along with four other algorithms. The tests of the five mapping algorithms leave a mixed result, where no algorithm can be singled out as the best. The four evaluation criteria showed that the algorithms generally behave expectedly, while the landmark test indicated that the spherical warp approach is more accurate than the rest of the tested algorithms. Choice of algorithm should depend on the study. Dependent on whether the preservation of intrinsic vertex configuration or the comparison of similar topographic areas is important, either the spherical warp or the ICF algorithm should be chosen, as these are respectively more accurate and preserve the most information. A combination of these algorithms could be a promising mapping method and should be investigated in the future. We showed that choice of mapping algorithm impacts the results drawn from statistical maps. However, considering the small number of subjects used here further testing should be carried out to confirm this. Finally, the number of different types of mapping algorithms tested is limited. Other types of mapping methods, such as methods based on diffeomorphic mapping, should also be compared in a future evaluation.

References

[1] L. Ahlfors. *Complex Analysis*. McGraw-Hill Science/Engineering/Math, 3rd edition, 1979.

[2] A. Almhdie, C. Léger, M. Deriche, and R. Lédée. 3D registration using a new implementation of the ICP algorithm based on a comprehensive lookup matrix: Application to

medical imaging. *Pattern Recognition Letters*, 28(12):1523–1533, 2007.

[3] D. R. Anderson, D. J. Sweeney, and T. A. Williams. *Statistics for business and economics*. South-Western College Publ., 8th edition, 2002.

[4] M. A. Audette, F. P. Ferrie, and T. M. Peters. An algorithmic overview of surface registration techniques for medical imaging. *Medical Image Analysis*, 4(3):201–217, 2000.

[5] P. J. Besl and N. D. McKay. A method for registration of 3-D shapes. *IEEE Trans. Pattern Analysis and Machine Intelligence*, 14(2):239–256, 1992.

[6] G. Chetelat and J. . Baron. Early diagnosis of alzheimer's disease: Contribution of structural neuroimaging. *NeuroImage*, 18(2):525–541, 2003.

[7] A. M. Dale, B. Fischl, and M. I. Sereno. Cortical surface-based analysis: I. segmentation and surface reconstruction. *NeuroImage*, 9(2):179–194, 1999.

[8] E. W. Dijkstra. A note on two problems in connexion with graphs. *Numerische Mathematik*, 1:269–271, 1959.

[9] S. F. Eskildsen and L. R. Østergaard. Active surface approach for extraction of the human cerebral cortex from MRI. *Lecture Notes in Computer Science*, 4191(II):823–830, 2006.

[10] J. Feldmar and N. Ayache. Rigid, affine and locally affine registration of free-form surfaces. *Int. J. Computer Vision*, 18(2):99–119, 1996.

[11] B. Fischl and A. M. Dale. Measuring the thickness of the human cerebral cortex from magnetic resonance images. *Proc. of the National Academy of Sciences of the USA*, 97(20):11050–11055, 2000.

[12] B. Fischl, M. I. Sereno, and A. M. Dale. Cortical surface-based analysis: II. Inflation, flattening, and a surface-based coordinate system. *NeuroImage*, 9(2):195–207, 1999.

[13] B. Fischl, M. I. Sereno, R. B. H. Tootell, and A. M. Dale. High-resolution intersubject averaging and a coordinate system for the cortical surface. *Human Brain Mapping*, 8(4):272–284, 1999.

[14] R. Goldenberg, R. Kimmel, E. Rivlin, and M. Rudzky. Cortex segmentation: A fast variational geometric approach. *IEEE Trans. Medical Imaging*, 21(12):1544–1551, 2002.

[15] G. L. Goualher, E. Procyk, D. Louis Collins, R. Venugopal, C. Barillot, and A. C. Evans. Automated extraction and variability analysis of sulcal neuroanatomy. *IEEE Trans. Medical Imaging*, 18(3):206–217, 1999.

[16] X. Gu, Y. Wang, T. F. Chan, P. M. Thompson, and S. . Yau. Genus zero surface conformal mapping and its application to brain surface mapping. *IEEE Trans. Medical Imaging*, 23(8):949–958, 2004.

[17] X. Han, D. L. Pham, D. Tosun, M. E. Rettmann, C. Xu, and J. L. Prince. CRUISE: Cortical reconstruction using implicit surface evolution. *NeuroImage*, 23(3):997–1012, 2004.

[18] P. J. Harrison. The neuropathology of schizophrenia. a critical review of the data and their interpretation. *Brain*, 122(4):593–624, 1999.

[19] M. K. Hurdal and K. Stephenson. Cortical cartography using the discrete conformal approach of circle packings. *NeuroImage*, 23(SUPPL. 1), 2004.

[20] L. Ju, M. K. Hurdal, J. Stern, K. Rehm, K. Schaper, and D. Rottenberg. Quantitative evaluation of three cortical surface flattening methods. *NeuroImage*, 28(4):869–880, 2005.

[21] S. K. June, V. Singh, K. L. Jun, J. Lerch, Y. Ad-Dab'bagh, D. MacDonald, M. L. Jong, S. I. Kim, and A. C. Evans. Automated 3-D extraction and evaluation of the inner and outer cortical surfaces using a laplacian map and partial volume effect classification. *NeuroImage*, 27(1):210–221, 2005.

[22] C. . Kao, M. Hofer, G. Sapiro, J. Stern, K. Rehm, and D. A. Rottenberg. A geometric method for automatic extraction of sulcal fundi. *IEEE Trans. Medical Imaging*, 26(4):530–540, 2007.

[23] F. Kruggel. Robust parametrization of brain surface meshes. *Medical Image Analysis*, 12(3):291–299, 2008.

[24] J. P. Lerch and A. C. Evans. Cortical thickness analysis examined through power analysis and a population simulation. *NeuroImage*, 24(1):163–173, 2005.

[25] L. M. Lui, Y. Wang, T. F. Chan, and P. Thompson. Landmark constrained genus zero surface conformal mapping and its application to brain mapping research. *Applied Numerical Mathematics*, 57(5-7 SPEC. ISS.):847–858, 2007.

[26] J. Nie, T. Liu, G. Li, G. Young, A. Tarokh, L. Guo, and S. T. C. Wong. Least-square conformal brain mapping with spring energy. *Computerized Medical Imaging and Graphics*, 31(8):656–664, 2007.

[27] A. Rangarajan, H. Chui, E. Mjolsness, S. Pappu, L. Davachi, P. Goldman-Rakic, and J. Duncan. A robust point-matching algorithm for autoradiograph alignment. *Medical Image Analysis*, 1(4):379–398, 1997. Cited By (since 1996): 45.

[28] M. E. Rettmann, X. Han, C. Xu, and J. L. Prince. Automated sulcal segmentation using watersheds on the cortical surface. *NeuroImage*, 15(2):329–344, 2002.

[29] Y. Shi, P. M. Thompson, I. Dinov, S. Osher, and A. W. Toga. Direct cortical mapping via solving partial differential equations on implicit surfaces. *Medical Image Analysis*, 11(3):207–223, 2007.

[30] M. Spjuth, F. Gravesen, S. F. Eskildsen, and L. R. Østergaard. Early detection of AD using cortical thickness measurements. *Progress in Biomedical Optics and Imaging*, 6512, 2007.

[31] D. Tosun, M. E. Rettmann, and J. L. Prince. Mapping techniques for aligning sulci across multiple brains. *Medical Image Analysis*, 8(3):295–309, 2004.

[32] M. Vaillant, A. Qiu, J. Glaunès, and M. I. Miller. Diffeomorphic metric surface mapping in subregion of the superior temporal gyrus. *NeuroImage*, 34(3):1149–1159, 2007.

[33] D. C. Van Essen, H. A. Drury, S. Joshi, and M. I. Miller. Functional and structural mapping of human cerebral cortex: Solutions are in the surfaces. *Proc. of the National Academy of Sciences of the USA*, 95(3):788–795, 1998.

[34] H. Xue, L. Srinivasan, S. Jiang, M. Rutherford, A. D. Edwards, D. Rueckert, and J. V. Hajnal. Automatic segmentation and reconstruction of the cortex from neonatal MRI. *NeuroImage*, 38(3):461–477, 2007.

[35] G. Zou, J. Hua, and O. Muzik. Non-rigid surface registration using spherical thin-plate splines. *Lecture Notes in Computer Science*, 4791(I):367–374, 2007.